JVI Journals.ASM.org

Experimental Infection of Cynomolgus Macaques (*Macaca fascicularis*) with Human Varicella-Zoster Virus

David O. Willer,[a,b] Aruna P. N. Ambagala,[a,b]* Richard Pilon,[d] Jacqueline K. Chan,[a] Jocelyn Fournier,[e] James Brooks,[f] Paul Sandstrom,[d] and Kelly S. MacDonald[a,b,c]

Department of Microbiology, Mount Sinai Hospital, Toronto, Ontario, Canada[a]; Clinical Sciences Division, Faculty of Medicine, University of Toronto, Toronto, Ontario, Canada[b]; Department of Immunology, University of Toronto, Toronto, Ontario, Canada[c]; National HIV and Retrovirology Laboratories, National Microbiology Laboratory, Public Health Agency of Canada, Ottawa, Ontario, Canada[d]; Scientific Services Division, Health Products and Food Branch, Health Canada, Ottawa, Ontario, Canada[e]; and National Laboratory for HIV Genetics, Public Health Agency of Canada, Ottawa, Ontario, Canada[f]

Varicella-zoster virus (VZV) is a member of the alphaherpesvirus family and the causative agent of chickenpox and shingles. To determine the utility of cynomolgus macaques (*Macaca fascicularis*) as a nonhuman primate model to evaluate VZV-based simian immunodeficiency virus/human immunodeficiency virus (SIV/HIV) vaccines, we experimentally inoculated 10 animals with the parental Oka (Oka-P) strain of VZV derived from MeWo or Telo-RF cells. VZV DNA could be detected in the lungs as late as 4 days postinfection, with replicating virus detected by shell vial culture assay in one case. Infection did not result in any overt clinical symptoms but was characterized by humoral and cell-mediated immunity in a time frame and at a magnitude similar to those observed following VZV vaccination in humans. The cell line source of VZV inoculum influenced both the magnitude and polyfunctionality of cell-mediated immunity. Animals mounted a vigorous anamnestic antibody response following a second inoculation 12 weeks later. Inoculations resulted in transient increases in $CD4^+$ T-cell activation and proliferation, as well as a sustained increase in $CD4^+$ T cells coexpressing CCR5 and $\alpha4\beta7$ integrin. In contrast to previous failed attempts to successfully utilize attenuated VZV-Oka as an SIV vaccine vector in rhesus macaques due to suboptimal infectivity and cellular immunogenicity, the ability to infect cynomolgus macaques with Oka-P VZV should provide a valuable tool for evaluating VZV-vectored SIV/HIV vaccines.

In recent years, there has been considerable interest in the development of novel replicating viral vectors in the advancement of HIV vaccines. Viral vector candidates are being sought that have the capacity to mimic the immunogenicity and protective capacity of a live attenuated human immunodeficiency virus/simian immunodeficiency virus (HIV/SIV) approach, while simultaneously offering an improvement in the margin of safety provided. While the nature of protection conferred by some experimental attenuated SIV vaccines has not been fully elucidated, viral persistence has been identified as one possible correlate of protection. Periodic and sustained viral reactivation in the context of herpesvirus reactivation may translate to continued antigen presentation, a requirement to induce and maintain an effector memory T-cell (T_{EM}) response. Herpesviruses, including cytomegalovirus (CMV) and varicella-zoster virus (VZV), are logical candidates in this pursuit.

VZV is a member of the alphaherpesvirus subfamily and is responsible for chickenpox and herpes zoster in humans. The virus establishes lifelong latency in terminal ganglia of the human host, with evidence of frequent subclinical reactivation and immunogenicity even in healthy individuals. This critical feature sets it apart from almost all vaccine vectors currently in testing for HIV, where severely attenuated or replication-deficient vectors are the standard (15). This capacity for lifelong infection of the vaccinee, together with the proven capacity for self-boosting of the vector (20), forms a novel paradigm for HIV vaccine development. A live, replicating attenuated vaccine strain of VZV (Oka strain) has been in use in humans since 1974 and is the basis of highly successful vaccination campaigns globally to reduce the incidence and severity of chickenpox and herpes zoster. Several other features make VZV an attractive vaccine vector, including the ability of VZV to prime both cellular and humoral immune responses and the observation that VZV (Oka), despite its administration as a subcutaneous or intramuscular vaccine, primes for mucosal antibody responses, a feature widely noted as a priority for HIV vaccine development (36). From a practical standpoint, the cloning of a VZV parental strain (Oka-P) as a bacterial artificial chromosome (BAC) (25) has allowed the possibility of extensive genetic manipulation of the VZV genome for the development of VZV derivatives expressing exogenous SIV/HIV antigens. VZV as a nonretroviral, nonintegrating persistent vaccine vector may well mimic features of successful attenuated SIV vaccines without the associated risk of the emergence of pathogenic vaccine virus variants.

VZV causes abortive infection in rodents and select nonhuman primates, while causing overt disease only in chimpanzees, gorillas, and humans (7, 24). There are reports demonstrating successful wild-type VZV infection in rhesus macaques (*Macaca mulatta*) (3, 29) that does not cause disease. Cynomolgus macaques (*Macaca fascicularis*) have been used increasingly along with the investigation of other species of monkeys for the evaluation of SIV/HIV vaccines due to the limited availability of Indian rhesus

Received 8 September 2011 **Accepted** 6 January 2012
Published ahead of print 18 January 2012
Address correspondence to Kelly S. MacDonald, kmacdonald@mtsinai.on.ca.
* Present address: Animal Diseases Research Institute, Canadian Food Inspection Agency, Lethbridge Laboratory, Lethbridge, Alberta, Canada.

doi:10.1128/JVI.06264-11

macaques following the export ban of April 1992 (28). Furthermore, SIV infection of cynomolgus macaques closely recapitulates the kinetics of HIV infection in humans, with a slightly more prolonged period of latency and disease progression than in rhesus macaques (35). This necessitates a somewhat longer monitoring period following infection, but meaningful differences in disease progression, set point viral load, and survival can be assessed, underscoring their potential usefulness for vaccine trials, particularly with disease progression endpoints. While VZV inoculation of cynomolgus macaques has been utilized previously to induce cytomegalovirus reactivation (26, 27), a clear understanding of the full extent of immunogenicity and replication, including the cellular tropism, growth kinetics, pathogenesis, and persistence of VZV in this species, is critical to effectively deliver and assess VZV-based SIV vaccine candidates in this species and to draw meaningful inferences about the applicability of the data to human vaccine trials of analogous HIV immunogens. Here, we assess the infectivity and immunogenicity following inoculation of 10 cynomolgus macaques using parental nonattenuated vaccine strain (Oka-P) of VZV.

MATERIALS AND METHODS

Virus preparation and cell lines. The parental strain (Oka-P) of varicella-zoster virus, cloned as a bacterial artificial chromosome (VZV-BAC) (25), was generously provided by Koichi Yamanishi (Osaka University, Japan). VZV-BAC was transfected into the human melanoma cell line (MeWo) to generate virus. The floxed BAC sequence remaining in the VZV genome was removed by serial passage of the virus in Vero-Cre (10) cells (gift from Sam Speck, Emory University). High-titer stocks were obtained by passage of the resultant VZV-Oka-P in either MeWo cells or in a telomerase-immortalized rhesus fibroblast cell line (Telo-RF) kindly provided by P. Barry at the University of California—Davis, CA (5, 17). The cells were maintained in Dulbecco's modified Eagle's medium (DMEM; Invitrogen) supplemented with 10% fetal bovine serum (FBS; Wisent Bioproducts, Quebec, Canada), 100 U/ml penicillin, and 100 μg/ml streptomycin (Sigma-Aldrich, St. Louis, MO). Viral titers were determined by standard VZV plaque assay on MeWo cells. The mean titer of VZV stocks obtained from MeWo cells was 8.5×10^6 PFU/ml, whereas Telo-RF-derived VZV yielded mean titers of 2×10^6 PFU/ml.

Animals. Ten adult male, colony-bred cynomolgus macaques (*Macaca fascicularis*) of mixed Indonesia/Mauritius lineage, with an average weight of 7.9 kg (range, 5.1 to 12.9 kg), were housed at the Animal Resources Division at the St. Frederick Banting Research Center (Ottawa, Canada) in accordance with regulations of the Health Canada Institutional Animal Care Committee. Serological testing revealed that the animals were free from infection with SIV, with type D simian retrovirus serotypes 1, 2, and 5, and with simian T-cell leukemia virus prior to initiation of the study. VZV-immunized animals were housed in a biosafety level 2+ (BSL-2+) containment facility in order to eliminate the theoretical risk of spread of the virus within the colony. Animals were monitored daily for food intake, stool consistency, and general well-being. Animals were routinely weighed, examined for external signs of enlarged lymph nodes, and monitored closely for clinical signs of VZV infection, including, but not limited to, vesicular lesions, fever, generalized malaise, and appetite suppression, concurrent to surveillance for secondary infections. The monkeys were randomly assigned to two vaccine groups ($n = 4$ per group), receiving VZV-Oka-P vaccinations and a control group ($n = 2$).

Inoculations. Virus inoculations and sampling procedures were conducted under anesthesia (10 mg/kg ketamine intramuscularly [i.m.]). High-titer stocks of MeWo or Telo-RF cell-associated VZV were thawed, centrifuged, and washed twice with DMEM supplemented with 2% FBS. The resultant pellet was resuspended in DMEM–2% FBS and passed several times through a 21-gauge needle to disrupt any cell aggregates. At the initial inoculation, animals received an intratracheal inoculation of 10 ml containing either MeWo-derived VZV (group 1, 1.8×10^7 PFU/animal), Telo-RF-derived VZV (group 2, 3×10^6 PFU/animal), or MeWo cell line control. Twelve weeks later, the animals received an intravenous inoculation derived from the other cell line from which they received the original inoculation. This was comprised of 10 ml of Telo-RF-derived VZV (group 1, 3.5×10^6 PFU/animal) or MeWo-derived VZV (group 2 and controls, 1×10^7 PFU/animal).

Sampling procedures. Single-cell suspensions were isolated from bronchoalveolar lavage (BAL) fluid. Anesthetized animals were instilled with 15 ml of phosphate-buffered saline (PBS) via an infant feeding tube (8-French diameter [Fr]) inserted into the endotracheal tube before being wedged into a secondary bronchus. The animals were rotated to favor diffusion of the saline, followed by elevation of the posterior of the animal to facilitate maximal recovery of the lavage fluids. The recovered fluid was centrifuged at 1,500 rpm for 7 min. The supernatant was discarded, and the cells were resuspended in 10 ml of R10 medium (RPMI medium supplemented with 10% FBS, 100 U/ml penicillin, and 100 μg/ml streptomycin) and filtered through a 70-μm-pore-size cell strainer. The cells were washed with R10 medium, centrifuged, resuspended in PBS containing 3% FBS, and stored on ice in preparation for immediate surface staining. Peripheral blood mononuclear cells (PBMCs) were obtained from whole-blood samples by Percoll density gradient separation as described previously (38).

Detection of VZV. Longitudinal analysis of acute varicella viremia was conducted using quantitative PCR and shell vial culture-based assays. Whole blood, bronchoalveolar lavage (BAL) fluid, and nasopharyngeal (NP) swabs were obtained between days 4 to 28 postinoculation (p.i.). Three NP swabs per animal were collected and agitated in virus transport medium (VTM). The swabs were discarded, and the VTM was subjected to centrifugation. The resultant pellet was resuspended in 400 μl of fresh VTM and divided in two for nucleic acid extraction or shell vial analysis. DNA was extracted from blood using a QIAamp DNA Blood Kit and from BAL fluid and NP samples using a DNeasy Blood and Tissue Kit (Qiagen, Valencia, CA). Quantitative PCR was conducted using an Artus VZV PCR kit (Qiagen, Hamburg, Germany) according to the manufacturer's protocols. Standards provided with the kit were run in duplicate, fluorescent values were averaged, and the standard curve generated was used to determine copy number in unknown test specimens. The dynamic range of the assay was 10 to 10,000 copies/μl. VZV-BAC diluted in double-distilled H_2O (ddH_2O) was also used as a positive control. All samples were run containing an internal control (IC) to ensure the absence of inhibitory factors in the PCRs. Results are reported as the number of VZV copies/μl based on the experimental BAL sample volume.

Shell vial cultures and direct fluorescent antibody (DFA) detection assays were used to assess the presence of replicating virus in PBMCs, BAL fluid, and NP samples. Shell vials containing confluent monolayers of a mix of African green monkey kidney cells (strain CV-1) and MRC-5 cells (called H & V cells) were obtained from Diagnostic Hybrids, Inc. (Athens, OH). Samples (200 μl each) were inoculated onto a freshly aspirated shell vial monolayer, centrifuged at room temperature for 15 min at $3{,}500 \times g$, and then supplemented with 1.5 ml of maintenance medium (Diagnostic Hybrids, Inc.). The shell vials were incubated at 36°C for 2 to 4 days while monitoring for cytopathic effects. The coverslips were then washed with PBS and fixed in 1 ml of 1:1 acetone-methanol mixture at room temperature for 10 min. The fixing solution was removed, and the coverslip was allowed to air dry. VZV was detected using immunofluorescent detection via DFA assay using a Merifluor VZV staining kit as per the manufacturer's instructions (Meridian BioSciences, Inc., Cincinnati, OH).

Detection of anti-VZV antibodies. Longitudinal analysis of antibodies directed against VZV was assessed in serum samples. An enzyme-linked fluorescent immunoassay (ELFA) varicella-zoster virus IgG test kit was used in accordance with standard operating procedures using a VIDAS System instrument (bioMérieux-Vitek Inc., MO).

VZV antigen and peptides. Crude VZV antigen was prepared from VZV-Oka-P-infected MRC-5 cells grown overnight at 37°C in DMEM

(Invitrogen) supplemented with 3% FBS (Wisent Bioproducts, Quebec, Canada), 100 U/ml penicillin, and 100 μg/ml streptomycin (Sigma-Aldrich, St. Louis, MO). The following day, the medium was removed, and the cells were washed once and fed with M199 medium (Invitrogen) and incubated at 37°C. When 80 to 90% cytopathic effect was observed, the cells were harvested by scraping the monolayer, and the cell suspension was subjected to a freeze-thaw cycle. The cell suspension was centrifuged at 2,000 × *g* for 10 min at 4°C, and the resultant supernatant was centrifuged at 35,000 × *g* for 90 min at 4°C. The supernatant was concentrated approximately 20-fold using Amicon Centriprep YM10 devices (Millipore) by centrifugation at 2,000 × *g* for 30 min at 4°C. Soluble control antigen was prepared in parallel from uninfected MRC-5 cells. Protein concentration was determined by Bradford assay. Samples were stored in single-use aliquots at −80°C.

Peptides (15-mers overlapping by 10 amino acids) representing VZV gene products, gI, gE, ORF4, and IE63 were obtained from Mimotopes (Victoria, Australia). Individual peptides were resuspended to 20 mg/ml in an 80% dimethyl sulfoxide (DMSO) solution in water and pooled based on their respective open reading frame (ORF). Peptide pools for gE, gI, ORF4, and IE63 were comprised of 124, 69, 260, and 89 peptides, respectively.

ELISPOT assay. VZV-specific gamma interferon (IFN-γ) secretion was measured by enzyme-linked immunosorbent spot (ELISPOT) assay as described previously (38), with some modifications. Freshly isolated PBMCs were routinely plated at 100,000 cells/well in a 100-μl total volume and stimulated in triplicate with VZV or control antigen (~350 μg/ml final). Stimulation with staphylococcal enterotoxin B (SEB) and M199 medium was used as a positive and negative control, respectively. Spots were enumerated using an automated reader system (CTL Analyzers, Cleveland, OH) employing ImmunoSpot, version 5.0, software. The numbers of IFN-γ-producing cells was calculated following background subtraction and were expressed as spot-forming cells (SFC)/10^6 PBMCs.

Flow cytometric analysis and intracellular cytokine assays. Routine complete blood counts and immunophenotyping were conducted as described previously (38). Briefly, 5,000 lymphocytes ($CD45^+$ [clone TU116]; low side scatter [SSC]) were acquired. T-cell populations were identified and enumerated by staining with antibodies directed against CD3 (SP34-2), CD4 (L200), and CD8 (RPA-T8). Natural killer (NK) cells ($CD3^-$) were identified following costaining with antibodies directed against CD16 (3G8) and CD56 (MY31). B cells were identified using the pan-B-cell marker CD20 (2H7). The absolute counts/μl were generated by the addition of Flow-Count Fluorospheres (Beckman Coulter) of known concentrations to the samples and calculated according to the following equation: (total number of cell events counted/total number of Flow-Count bead events counted) × (Flow-Count assay concentration).

For assessment of activation levels and potential target cell populations, cryopreserved PBMCs were thawed and isolated over a Percoll (GE Healthcare Bio-Sciences, NJ) gradient as described previously (38). The cells were resuspended to 2.5 × 10^6/ml in R10 medium, and 500,000 cells were plated per well in a V-bottom 96-well plate. Prior to surface staining, the cells were stained with an amine-reactive live/dead stain (Invitrogen) according to the manufacturer's protocol. The cells were washed twice with fluorescence-activated cell sorting (FACS) buffer (PBS–3% FBS) and stained for surface markers using the following antibodies: CD3 (clone SP34-2), CD4 (L200), CD8 (RPA-T8), CD25 (BC96), HLA-DR (G46.6), CCR5 (3A9), and α4β7 (rhesus recombinant antibody from the NIH Nonhuman Primate Reagent Resource). Stained cells were washed extensively and then fixed and permeabilized using Cytofix/Cytoperm solution (BD Biosciences) according to established protocols. Intracellular cytokine staining was conducted in Perm/Wash solution (BD Biosciences) using antibodies directed against CD69 (FN50) and Ki67 (B56). Cells were washed twice with Perm/Wash solution and resuspended in FACS buffer for immediate data acquisition using a BD LSR II flow cytometer. Thirty thousand gated T-lymphocytes (viable $CD3^+$ $CD4^+$) were collected and analyzed using FlowJo software (Treestar, OR). Fluorescence minus one (FMO) or isotype controls were used to delineate positive events. Basic statistical differences of mean values between time points with respect to activation markers and were assessed using a paired-samples *t* test (SSPS software, version 19).

For surface staining and intracellular cytokine analysis (ICS) by flow cytometry, lymphocytes were prepared as above and rested overnight at 37°C. The following day, the cells were stimulated with peptides (2.5 μg/ml/peptide) in the presence of costimulatory molecules CD28 (CD28.2) and CD49d (9F10) in FACS buffer. Following incubation at 37°C for 1.5 h, brefeldin A and monensin (5 μg/ml each) were added, and the incubation was allowed to continue for an additional 5.5 h. The reaction was stopped with the addition of 20 μl of EDTA (20 mM in PBS) and incubated at room temperature for 15 min. Cells were stained with a viability dye and subsequently with surface markers CD3 (clone SP34-2), CD8 (RPA-T8), and CD4 (L200). Intracellular cytokine staining was conducted as above using antibodies directed against IFN-γ (clone B27), tumor necrosis factor alpha ([TNF-α] MAb11), interleukin-2 ([IL-2] MQ1-17H12), CD107a (H4-A3), and MIP-1β (24006) at 4°C. Cells were acquired immediately using a BD FACS Canto II flow cytometer. Data analysis was performed using FlowJo software (Treestar, OR) and SPICE (version 5.2 [http://exon.niaid.nih.gov/spice/]). SEB- and DMSO-treated cells acted as positive and negative controls, respectively. Results are represented as background subtracted for each individual animal at any given time point, in addition to subtraction of any background responses present at baseline. Basic statistical differences of mean values between groups with respect to polyfunctional cytokine secretion were assessed using Student's *t* test following Levene's test for equality of variances (SSPS software, version 19).

RESULTS

Clinical observations. Two groups of experimental animals were inoculated intratracheally with cell-associated VZV derived from MeWo (group 1) or Telo-RF (group 2) cells as described in Materials and Methods. A third group of control animals received an intratracheal inoculation of uninfected MeWo cells prepared in parallel. Twelve weeks following the initial inoculation, the animals received an intravenous inoculation derived from the other cell line from which they had originally received an inoculation. The control group received MeWo-derived VZV at this time. Animals were examined clinically and hematologically monitored for signs of illness typically associated with VZV infection in humans. As expected, none of the animals showed evidence of vesicular rash, and both sources of inoculum were tolerated well by the animals. A summary of clinical findings can be found in Table 1.

Flow cytometry was used to clinically monitor both the absolute numbers and relative percentages of lymphocyte subsets ($CD3^+$ $CD4^+$ T cells, $CD8^+$ T cells, B cells, and NK cells) over the course of the study (Fig. 1). There were no statistically relevant differences between the vaccine and control groups. The initial inoculation resulted in a relative increase in lymphocyte counts, with the exception of B cells that peaked 10 days postinoculation and quickly resolved to baseline. The expansion was most pronounced in the T-cell subsets, with both $CD4^+$ and $CD8^+$ cells displaying similar expansions in numbers (Fig. 1A). The second inoculation resulted in a relative and transient decrease in lymphocyte subsets. The various proportions of each lymphocyte subset remained relatively constant throughout the study (Fig. 1B).

Detection of VZV. Our efforts to detect VZV in the mucosa and peripheral circulation included both quantitative PCR and shell vial coculture assays. Bronchoalveolar lavage samples were collected at days 4, 10, 21, and 28 postinoculation, with whole-blood samples (days 10, 15, and 21 p.i.) and nasopharyngeal (NP)

TABLE 1 Clinical observations following VZV inoculation

Factor	Presence of factor by animal and inoculation regimen[a]																			
	Group 1								Group 2								Controls			
	C88-117M		C87-009M		C91-080M		C04-019M		C89-100M		C95-073M		C91-078M		C04-015M		C87-103M		C93-093M	
	A	B	A	B	A	B	A	B	A	B	A	B	A	B	A	B	A	B	A	B
Pyrexia[b]	−	−	+	−	−	−	−	−	−	+	−	−	−	−	−	−	−	−	−	−
Anorexia[c]	−	−	−	−	−	+	−	−	−	−	−	+	−	−	−	+	−	+	−	−
Lymphadenopathy[d]	−	−	−	−	+	+	−	−	−	−	−	−	−	−	−	−	−	−	−	−
Abnormal stool/urine[e]	−	−	−	−	−	−	−	−	−	−	−	+	−	−	−	−	−	+	−	−
Coryza[f]	−	−	+	−	−	−	−	−	−	−	−	−	−	−	−	−	−	−	−	−

[a] Animals were monitored daily for food intake, stool consistency, and general well-being. Animals were routinely weighed, examined for external signs of enlarged lymph nodes, and monitored closely for clinical signs of VZV infection, including, but not limited to, vesicular lesions, fever, generalized malaise, and appetite suppression, concurrent to surveillance for secondary infection. A, initial intratracheal inoculation at week 0; B, intravenous inoculation at week 12. Animal C95-073M coughed immediately after receiving the first inoculation (A) and thus did not receive the full dose.

[b] Increased body temperature of ≥38.4°C.

[c] Lack of appetite exceeding 24-h period following general anesthesia.

[d] Lymph nodes of >1 cm in any diameter.

[e] Diarrhea, blood in stool, hematuria, or hematochezia.

[f] Nasal discharge.

swabs also obtained (day 15 p.i.). PCR quantitation of VZV in BAL samples revealed measurable levels of VZV in the lungs 4 days following inoculation (Table 2). Group 1 demonstrated a mean level of 503 copies/μl, with group 2 having a mean of 41 copies/μl. Animal C95-073M was not included in the preceding analysis as it coughed while receiving the inoculum and thus did not receive a full dose, likely accounting for the lower levels of detectable VZV in the lungs at day 4. Falling below the validated assay cutoff, viral DNA was detectable in many cases out to 28 days postinoculation (Table 2). We were unable to detect VZV by PCR in either the blood or NP samples. Of note, the DNA yield from the NP swabs was very low and likely precluded any chance of viral detection. Furthermore, we were unable to detect any VZV DNA by PCR following the second inoculation at five similar time points assessed between days 4 and 28 postinoculation.

Shell vial viral coculture of BAL samples on H & V cell monolayers (MRC-5–CV-1 mix), followed by DFA, demonstrated the presence of infectious virus in the lungs of animal C91-080M at day 4 postinfection (data not shown). We were unable to detect replicating virus in any other animals at this or subsequent time points.

CD4$^+$ T-cell activation and CCR5 and $\alpha4\beta7$ surface expression. The only previous attempt to utilize VZV as a viral vector for nonhuman primate evaluation of SIV/HIV vaccines was an apparent failure, resulting in increased SIV replication and accelerated SIV disease progression in vaccinated rhesus monkeys (29). To

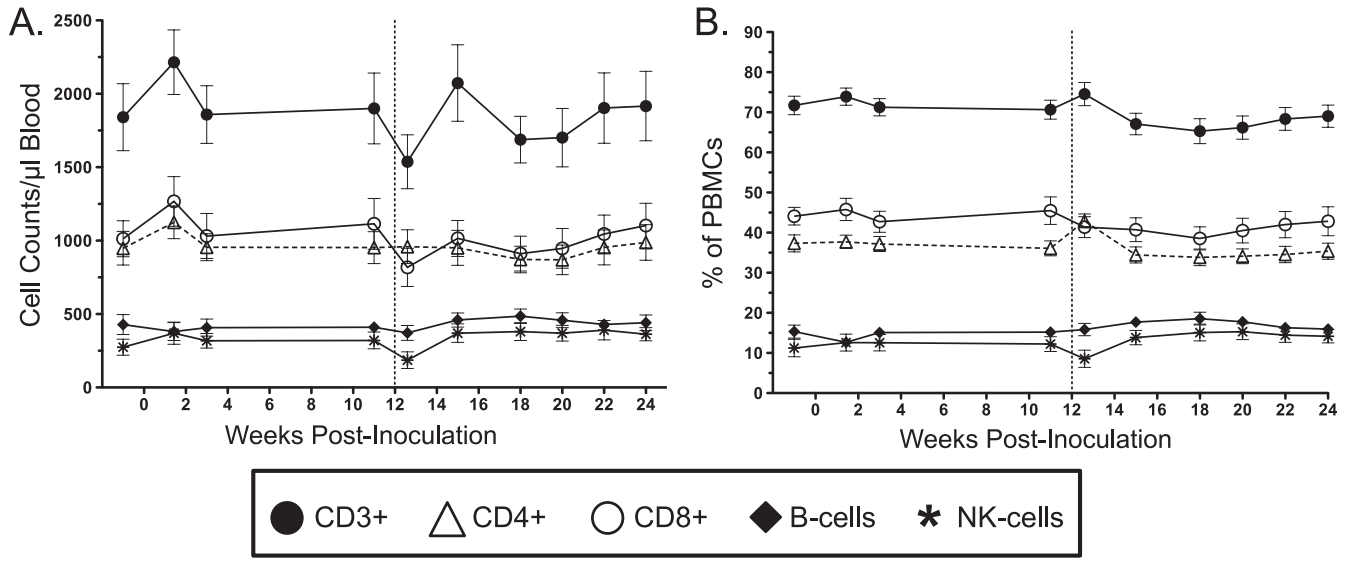

FIG 1 Quantitative immunophenotyping of peripheral lymphocyte subsets based on flow cytometric analysis of surface markers. (A) Enumeration of absolute numbers of T cells (CD3$^+$, CD3$^+$ CD4$^+$, and CD3$^+$ CD8$^+$), B cells (CD20$^+$) and NK cells (CD3$^-$ CD16$^+$ CD56$^+$) per μl of blood represented as the mean ± standard error of the mean for all animals. (B) The relative distribution of each cell subset is listed as a percentage of total PBMCs. The vertical hashed line indicates the time of intravenous inoculation.

TABLE 2 Detection of VZV

Sampling day	Amt of virus detected by PCR (no. of VZV copies/μl)[a]									
	Group 1				Group 2				Controls	
	C88-117M	C87-009M	C91-080M	C04-019M	C89-100M	C95-073M[b]	C91-078M	C04-015M	C87-103M	C93-093M
Day 4	708	1179	118	7	59	0.2	48	16	−	−
Day 10	0.34	−	0.45	0.23	−	0.24	−	0.05	−	−
Day 21	0.38	−	0.003	−	−	−	−	0.02	−	−
Day 28	0.02	0.004	0.3	−	−	−	−	0.004	−	−

[a] VZV DNA from BAL samples was amplified via quantitative PCR at the indicated days after initial inoculation. A shell vial culture-based assay was used to detect replicating VZV at day 4 postinoculation. Standards provided with kit were run in duplicate, fluorescent values were averaged, and the standard curve generated was used to determine copy number of unknown test specimens. The dynamic range of the assay was 10 to 10,000 copies/μl; values of <10 copies/μl fall below the validated limit of detection of the assay. All specimens were run containing internal controls in order to identify inhibitory factors in the PCR, and no PCR inhibition was seen with the specimens. For all animals except animal C91-080M, the results of shell vial and DFA assays were negative.

[b] Animal C95-073M coughed immediately after receiving the initial inoculation and thus did not receive the full dose.

assess the role of VZV inoculation on critical parameters of SIV infection and disease pathogenesis, levels of systemic immune activation on $CD4^+$ T cells were examined longitudinally from cryopreserved PBMC samples. We also evaluated the impact of VZV inoculations on surface expression of the HIV/SIV coreceptor CCR5 (CD195) (13, 22) and integrin $\alpha4\beta7$ on $CD4^+$ T cells. Integrin $\alpha4\beta7$ has been shown to act as a receptor and signaling molecule facilitating HIV and SIV infection (1), and cells which express elevated levels of $\alpha4\beta7$ are preferential targets for acute SIV infection (16, 37). During the course of our analysis, there were no statistically significant differences between any of the two experimental or control groups, and thus the statistical analysis was conducted on all of the samples combined. The primary inoculation resulted in an increase in the early activation marker CD69 (8) and Ki67, a marker of cellular proliferation (9). This response peaked at 2 weeks postinoculation (P values of <0.000 and 0.002, respectively) and remained elevated at the second inoculation at week 12 (P values of <0.000 and 0.009, respectively) (Fig. 2A). The late (CD25) and very late (HLA-DR) activation markers (8) demonstrated a similar increase with delayed kinetics, peaking at 3 weeks postinoculation (Fig. 2B). The percentage of cells expressing CCR5 and cells coexpressing both CCR5 and $\alpha4\beta7$ were similarly increased, with peak responses at weeks 2 ($P = 0.021$) and 3 ($P = 0.005$), respectively. Cells coexpressing the CCR5 and $\alpha4\beta7$ remained elevated until the second inoculation ($P = 0.005$) (Fig. 2C). The second inoculation had only a modest effect on cellular activation levels with only a transient increase in cellular proliferation (Ki67) ($P = 0.018$) and decreases in CD25 ($P < 0.000$) and HLA-DR ($P = 0.047$) levels. The number of cells coexpressing CCR5 and $\alpha4\beta7$ continued to decline following the second inoculation. By study termination at week 24, all of the activation markers had returned to baseline levels. Importantly, the level of $CD4^+$ T cells coexpressing CCR5 and $\alpha4\beta7$ remained elevated ($P = 0.033$) (Fig. 2C).

Antibody response to VZV. Serum levels of anti-VZV IgG antibodies were evaluated weekly for the first 16 weeks of the study and subsequently biweekly until the end of the study (Fig. 3). Serum antibodies were measurable as early as 1 week postinoculation (animal C04-019M), with all experimental animals displaying positive responses (optical density [OD] of >0.9) by 21 days, with the exception of animal C95-073M, which did not receive a full dose due to a coughing episode at the time of inoculation (Fig. 3). Animal C91-080M displayed a rapid increase in antibody levels that peaked between weeks 2 and 4 postinoculation. For the remaining animals, antibody levels peaked at approximately 4 weeks postinoculation, including animal C95-073M, whose enzyme-linked immunosorbent assay (ELISA) readings were subsequently consistent with a positive response. There was a trend toward increased mean peak antibody responses between group 1 (OD of 3.78) and group 2 (OD of 3.09). Following peak, responses de-

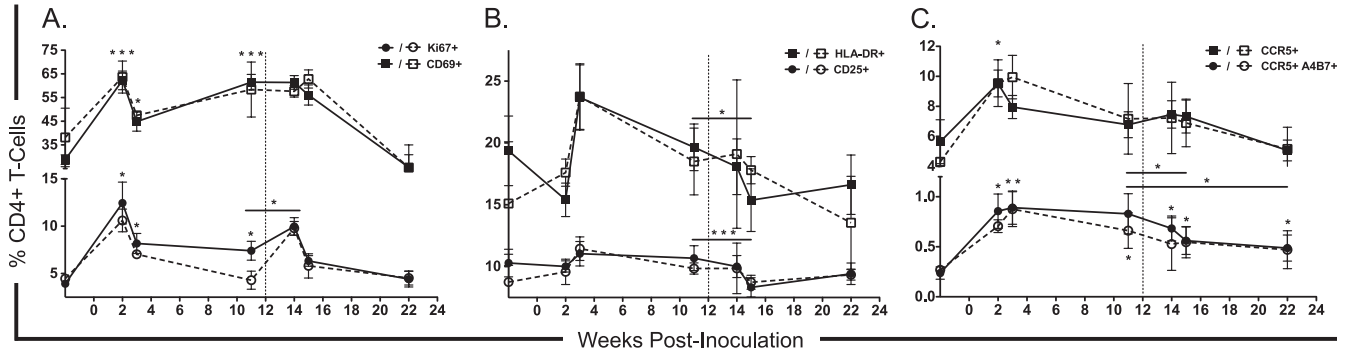

FIG 2 Longitudinal evaluation of peripheral $CD4^+$ T-cell activation, proliferation, and CCR5 and integrin $\alpha4\beta7$ surface expression. Percentages of $CD4^+$ T cells expressing the early activation marker CD69 or proliferation marker Ki67 (A), late activation markers CD25 or HLA-DR (B) are shown as well as percentages of cells expressing CCR5 or coexpressing CCR5 and integrin $\alpha4\beta7$ (C). Data points are represented as the mean ± standard error of the mean. Solid symbols and lines represent groups 1 and 2 combined, and the control group is represented with open symbols and hashed lines. Statistical significance was determined between time points for all animals combined (*, $P \leq 0.05$; **, $P \leq 0.001$; ***, $P \leq 0.0001$). The vertical hashed line indicates the time of intravenous inoculation.

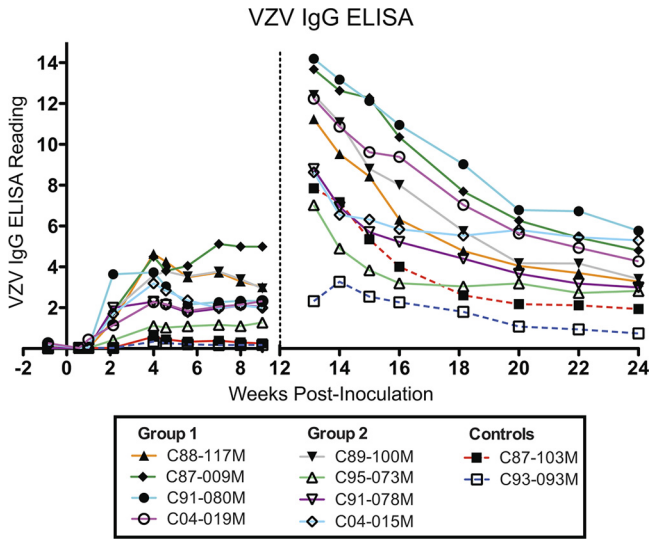

FIG 3 Longitudinal assessment of humoral immunity to VZV. VZV-specific IgG responses were evaluated by weekly VZV IgG ELISA of serum samples. Data points represent a single test per time point. The assay was conducted following stringent standard operating procedures used for clinical evaluation of anti-VZV titers in hospital patients. The ELISA readings provide a semiquantitative assessment of antibody titers. Time zero represents the initial intratracheal inoculation, and the vertical hashed line indicates the time of intravenous inoculation 12 weeks thereafter.

clined and reached a steady state in most cases by 5 to 6 weeks, with the exception of animals C87-009M and C095-073M, which continued to increase until the second inoculation. Control animals were consistently negative throughout the first 12 weeks of analysis, as expected.

Following the intravenous inoculation at 12 weeks, all animals previously exposed to VZV mounted an extremely rapid and robust anamnestic response that peaked within 10 days postinoculation. There was a trend toward greater peak ELISA responses between group 1 and group 2 (mean OD of 12.84 versus 6.15). Antibody levels followed a steady decline over the following 12 weeks of study reaching a nominal level above that seen prior to the second inoculation (Fig. 3). Of note, the two control animals receiving MeWo-derived VZV inoculum via the intravenous route for the first time at week 12 demonstrated disparate antibody response profiles. Animal C93-093M responded in a manner very similar to the experimental animals receiving VZV in the primary inoculation. This animal demonstrated a modest increase in anti-VZV IgG, which peaked 2 weeks following inoculation and decreased moderately thereafter. The other control animal (C87-103M) mounted a very fast and robust antibody response demonstrating a peak response within the first 10 days with a subsequent rapid decline (Fig. 3).

Cell-mediated immunity to VZV. Cell-mediated immunity to VZV was assessed by IFN-γ ELISPOT assay in response to incubation of PBMCs with preparations of crude VZV antigen. VZV-specific responses were assessed biweekly with initial detection of responses in groups 1 and 2 at 6 weeks after primary inoculation (Fig. 4A). Both groups exhibited peak T-cell responses at week 10. The second inoculation at week 12 did not result in a significant boost in IFN-γ-secreting cells. Control animals that received intravenous inoculation at 12 weeks demonstrated anti-VZV responses with a comparable magnitude but with delayed kinetics to those seen following primary inoculation (Fig. 4A).

The use of VZV as an HIV vaccine vector likely requires the induction of robust $CD8^+$ and $CD4^+$ T-cell responses. As such, a flow cytometric approach was taken to examine the capacity of these infections to induce polyfunctional $CD4^+$ and $CD8^+$ T-cell responses by assessing the ability to respond to various VZV peptide pools as measured by cytokine secretion (IFN-γ, TNF-α, IL-2, and MIP-1β) and CD107a (a marker of degranulation) expression (Fig. 4B). As measured at week 10, just prior to the second inoculation and at the peak of cell-mediated IFN-γ production, both groups of animals presented with responses against VZV peptide pools. Although not statistically significant, the animals in group 2 receiving Telo-RF-derived virus displayed elevated $CD4^+$ and $CD8^+$ T-cell responses compared to animals that received MeWo-derived VZV (Fig. 4A). Furthermore, there was an increased degree of polyfunctional $CD8^+$ T-cell responses in Telo-RF-VZV recipients expressing either five or four cytokines simultaneously ($P = 0.03$ or $P = 0.093$, respectively) (Fig. 4B). Polyfunctional cytokine secretion was also assessed 12 weeks after the second inoculation. This second VZV exposure resulted in more dramatic boosting of the immune responses in group 1 animals that initially received MeWo-derived VZV and were boosted with Telo-RF-VZV, as well as increased four-function $CD8^+$ T-cell responses ($P = 0.002$) than in group 2 animals (Fig. 4B). MeWo-derived VZV did not result in significant boosting of T-cell immunity. Notably, irrespective of which series of primary and secondary inoculations the animals received, the polyfunctionality of the $CD4^+$ T-cell immune response was increased following the boost with more five-function responses in both group 1 ($P = 0.062$) and group 2 ($P = 0.042$) animals than at week 10 (Fig. 4B). Group 1 animals also presented with an increase in four-function $CD8^+$ T-cell responses ($P < 0.001$) (Fig. 4B). There was no statistically significant difference in magnitude or polyfunctionality of T-cell responses when an intratracheal MeWo-VZV inoculation at week 10 (group 1) was compared to an intravenous MeWo-VZV inoculation at week 24 (controls) although there was a trend toward decreased monofunctional responses and an increase in five-function responses ($P = 0.079$).

DISCUSSION

Varicella-zoster virus is a highly species-specific pathogen that causes overt disease only in humans, chimpanzees, and gorillas (7, 24). Cynomolgus macaques (*Macaca fascicularis*) have previously been examined for their susceptibility to VZV infection with little evidence of infection or immunity (26, 27). However, these earlier studies utilized inoculation of low doses of VZV strains via nonphysiological routes and did not assess the potential for VZV to induce cellular immunity. In our effort to recapitulate successful heterologous infection of cynomolgus monkeys, we chose to employ the nonattenuated parental strain of VZV (Oka-P). Our rationale was such that a more virulent strain may have an improved ability to overcome the species specificity barrier. Takahashi and colleagues developed the first human herpesvirus vaccine against VZV in the 1970s (32, 34). The parental Oka strain (Oka-P) was attenuated by serial passage in cell culture (30, 31) to generate the vaccine strain (Oka-V) which is the basis for current vaccines against VZV (Varivax and Zostavax [Merck] and Varilrix [GlaxoSmithKline]). High-titer VZV was grown in the human melanoma cell line (MeWo) and Telo-RF cells. Telo-RF cells are a

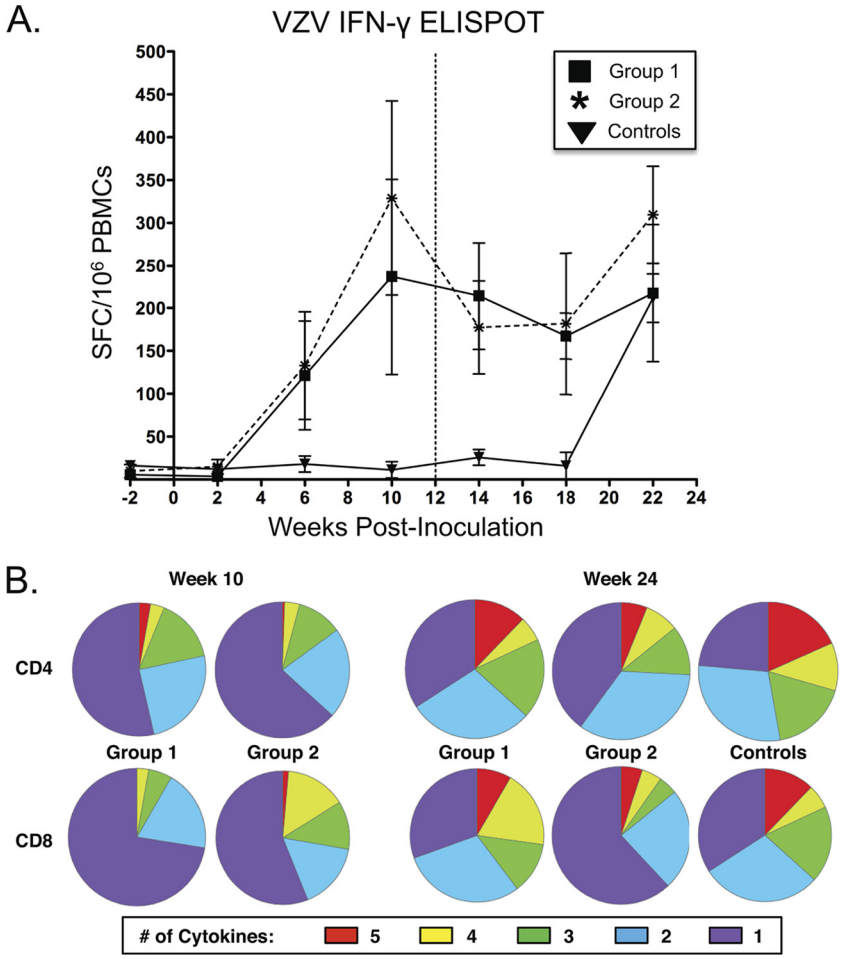

FIG 4 VZV-specific cell-mediated immunity. (A) IFN-γ ELISPOT assay responses in PBMC preparations following stimulation with whole VZV antigen. Data points represent the background-subtracted mean response from at least three replica wells on each of two duplicate plates per experiment with error bars indicative of the standard error of the mean. Responses are indicated as the numbers of IFN-γ-producing cells as SFC per million PBMCs. Time zero represents the initial intratracheal inoculation, and the vertical hashed line indicates the time of intravenous inoculation 12 weeks later. (B) Cytokine profile of T-cell immunity following stimulation with peptide pools spanning the VZV IE63, ORF4, gI, and gE proteins as measured by intracellular cytokine secretion of IFN-γ, MIP-1β, TNF-α, IL-2, and CD107a. Boolean gating on FlowJo software was used to determine the extent of coincident cytokine secretion. Pie charts generated using SPICE software represent the mean multifunctional responses directed against all peptide pools for each group.

telomerase-immortalized cell line derived from rhesus macaque fibroblasts (6, 17). We reasoned that some degree of tissue culture adaptation in a macaque cell line derived from a closely related species might allow for more effective infection and drive a more efficient establishment of a latent infection. The viral titers that we were able to generate from VZV-infected Telo-RF cells were slightly less than those obtained from passage in MeWo, likely due only to limited serial passage. To our knowledge, this is the first report demonstrating that VZV can be propagated in this cell line.

VZV is naturally acquired via aerosol or airborne droplet inoculation of the respiratory mucosa, with the lung and reticuloendothelial system as the initial sites of viral replication and expansion. Thus, our animals were inoculated intratracheally with the aim of delivering a significant viral inoculation to susceptible sites to maximize the rapidity and extent of VZV infection. VZV infection of humans proceeds through two phases of transient viremia (reviewed in reference 14). An initial phase of subclinical viremia occurs approximately 4 to 6 days following exposure as the virus expands in regional lymph nodes. A second, more pronounced viremia occurs between 10 and 21 days after infection. Infection of susceptible nonhuman primates, such as African green monkeys with simian varicella virus (SVV), induces a transient viremia peaking 7 to 10 days following experimental intratracheal inoculation (12). As such, we focused our attempts to detect virus within the first 28 days following experimental inoculation by assessing both mucosal and systemic sites. Quantitative PCR was sufficiently robust to detect VZV DNA in BAL samples collected 4 days postinoculation, which, although below the validated assay cutoff, was still detectable in a subset of animals 28 days later. The significant levels of VZV detectable in BAL samples at day 4 are likely attributable to residual inoculum and insufficient bronchial clearance although our results are similar in both magnitude and kinetics to those demonstrated following intrabronchial infection of rhesus macaques with SVV (23). Although the respiratory mucosa and lung tissue are the sites of initial infection, VZV is rarely detectable in these tissues (11, 14, 18). However, replicating virus was successfully detected in the BAL fluid of one animal at this time point using viral coculture and quantitative PCR techniques,

suggesting either that the lung is mildly permissive to VZV replication or that the local environment allows for prolonged maintenance of live virus associated with the inoculation. PBMC samples were negative for VZV at all time points assessed by both PCR and viral coculture methods. This is not surprising, as in humans viremia is transient, and only a small subset of cells (~0.01 to 0.001%) are infected with VZV even at the time of peak viremia (18, 19, 21). In most cases, successful attempts to detect VZV are aided by the visible presence of rash, but even in those cases, VZV-infected PBMCs are usually undetectable 24 to 72 h thereafter (19), highlighting the difficulties in following VZV viremia even in the natural host.

VZV infection of humans manifests itself with various prodromal symptoms, including fever, general malaise, headaches, anorexia, and loss of appetite that precede the development of maculopapular exanthema. Fever associated with VZV infection in humans is usually mild and often less than 38.6°C (2). Based upon observations that VZV does not produce overt disease in monkey species tested to date, we did not expect any significant pathogenesis following our manipulations. In general, the inoculations were well tolerated, with some animals presenting combinations of mild fever, transient weight loss, enlarged inguinal lymph nodes, and nasal discharge. The second challenge induced anorexia and sustained appetite suppression in a subset of animals, with some evidence of fever and enlarged lymph nodes. The clinical manifestations and kinetics of these observations are consistent with those seen in humans with mild disease. As anticipated, none of the animals developed any vesicular lesions.

Natural infection and vaccination with VZV lead to the induction of a durable systemic antibody response, with the elicitation of IgM, IgG, and IgA antibodies. IgM and IgG antibodies can be detected as early as 6 and 9 days postinfection, respectively, after the onset of symptoms (4), with IgG antibodies typically maintained beyond age 60 (33). In our current study, serological monitoring of antibody responses revealed measurable IgG as early as 2 weeks postinoculation at levels comparable to those seen following vaccination in humans and in rhesus macaques (29) infected with VZV. IgG responses did not show any appreciable decrease over the subsequent 12 weeks prior to the second inoculation. The second inoculation resulted in an anamnestic immune response. It was difficult to gain insight into the roll of the inoculation route with respect to the development of anti-VZV antibody responses as the two control animals that received an intravenous inoculation presented with different antibody response profiles.

As a measure of cell-mediated immunity, we assessed IFN-γ responses via stimulation with crude VZV antigens. Initial antiviral responses were detected in the periphery by 6 weeks postinoculation and appeared to peak approximately 10 weeks postinoculation and thereafter began to wane. The onset of cell-mediated immunity is somewhat delayed compared to VZV infection of humans in which VZV-specific T-cell responses occur rapidly with detection as early as 24 to 72 h postexanthema, or the equivalent of 2 to 4 weeks postinfection. This likely resulted from the high degree of species specificity imparted in the effort to infect cynomolgus monkeys with human VZV. Although animals in group 1 received a higher initial dose of VZV, the cellular immune responses between the two experimental groups were not significantly different though larger experimental numbers may have improved statistical relevance. Control animals receiving VZV via intravenous administration demonstrated delayed kinetics in the development of cell-mediated immunity but generated significant responses by 10 weeks. This delay in kinetics compared to intratracheal inoculation may be due in part to the extremely high dose and nonphysiological route in combination with species specificity constraints. ELISPOT assays do not differentiate between CD4- and CD8-based responses; therefore, we conducted a more thorough analysis examining antiviral responses by flow cytometry with an assessment of various cytokine levels (CD107a, IFN-γ, TNF-α, IL-2, and MIP-1β) following stimulation with peptide pools derived from a subset of VZV proteins, including IE63, ORF4, gE, and gI. Of particular interest is the observation that the polyfunctionality of the T-cell response was influenced by the cell type in which the inoculum was derived. Although given in a lower dose due to limitations in generating high-titer stocks, VZV that was grown in a rhesus macaque fibroblast cell line (Telo-RF) consistently produced elevated cytokine levels in both $CD4^+$ and $CD8^+$ T-cell compartments, with increased polyfunctionality demonstrated by $CD8^+$ T cells following the initial infection. Telo-RF-derived VZV also presented with a dramatically improved ability to increase both the magnitude and polyfunctional nature of the T-cell response when used as a boost. Although the VZV was only minimally passaged in Telo-RF cells, it is possible that some degree of growth adaptation occurred allowing for improved replicative capacity in the closely related macaque species. To our knowledge, the observation that tissue culture conditions impart or select for properties in a virus or vector that can act as immunomodulators has not been demonstrated previously.

An initial challenge to the concept of VZV as a vaccine vector for HIV came from Staprans and colleagues, who showed a lack of protection of rhesus macaques from heterologous SIV challenge by immunization with a single HIV *env* gene recombinant $VZV_{OKA\text{-}V}$ vaccine virus (29). Upon SIV challenge only 1 month after vaccination, the immunized animals had a more pronounced disease course than unimmunized animals, which was ascribed to the increased presence of activated SIV-specific $CD4^+$ T cells, which are a known target and reservoir for viral replication, in the absence of an effective cellular immune response. The investigators postulated that this population of primed and acutely boosted cells acted as an available reservoir for extremely rapid replication of the challenge virus over and above the level seen in naive animals lacking SIV-specific $CD4^+$ T cells. Our results demonstrating an increase in cellular activation and cell proliferation would support this notion. Furthermore, we have shown that there is a sustained increase in $CD4^+$ T cells coexpressing CCR5 and $\alpha4\beta7$, thus increasing the frequency of potential target cells for HIV or SIV infection. However, in our current study, we were unable to attribute any of these observations specifically to VZV. Rather, the changes that we noted were uniformly present across both the experimental and control groups and likely attributable to components of the cell-associated inoculum. VZV is inherently difficult to produce as a cell-free virus, and as both our group and Straprans et al. (29) used cell-associated preparations, it is clear that further studies are required to determine the potential for VZV as an HIV vaccine vector following vaccinations with cell-free preparations of VZV.

The clinical safety record and licensure of VZV vaccines in many countries dramatically decrease the barriers to moving forward with VZV-based HIV vaccines in human trials if ongoing macaque SIV challenge trials in our laboratory show evidence of safety and efficacy. Importantly, these studies clearly demonstrate

that a variety of factors, including dose, timing, route of inoculation, and the source of virus for inoculation can heavily influence the infectivity and immunity generated. Clearly, future studies will be needed to establish the optimal regimen with respect to route, dose, and utility of prime/boost methods and to determine whether cell-free preparations can impart similar or improved immunogenicity and infection. Furthermore, studies directed at examining both peripheral and effector T-cell memory function will be important in the context of using VZV as an HIV/SIV vaccine vector. Only recently has the field begun to examine the unique properties of herpesviruses, each perhaps with their own inherent potential to act as innate immune adjuvants in and of themselves and elicit the type of mucosally directed balanced immune response likely required in a successful HIV vaccine.

ACKNOWLEDGMENTS

We thank Koichi Yamanishi (Osaka University, Japan) for the VZV-BAC (Oka-P), Sam Speck (Emory University, Atlanta, GA) for Vero and Vero-Cre cell lines, and Peter Barry and William Chang (University of California, Davis) for Telo-RF cells. We sincerely thank the veterinary and technical staff at the NHP colony of Health Canada.

D.O.W. was supported by a Junior Investigator Development Award from the Ontario HIV Treatment Network (OHTN). A.P.N.A. and K.S.M. also received funding from the OHTN as a postdoctoral fellowship and career scientist award and as the OHTN endowed chair, respectively. This research was funded in part by the Canadian Institutes of Health Research and the Canadian Foundation for AIDS research.

REFERENCES

1. **Arthos J, et al.** 2008. HIV-1 envelope protein binds to and signals through integrin $\alpha4\beta7$, the gut mucosal homing receptor for peripheral T cells. Nat. Immunol. **9**:301–309.
2. **Arvin AM.** 1999. Chickenpox (varicella), p 96–110. *In* Wolff MH, Schunemann S, Schmidt A (ed), Varicella-zoster virus. Molecular biology, pathogenesis and clinical aspects, vol 3. Karger, Basel, Switzerland.
3. **Asano Y, et al.** 1984. Immunogenicity of wild and attenuated varicella-zoster virus strains in rhesus monkeys. J. Med. Virol. **14**:305–312.
4. **Bogger-Goren S, et al.** 1982. Antibody response to varicella-zoster virus after natural or vaccine-induced infection. J. Infect. Dis. **146**:260–265.
5. **Chang WL, Barry PA.** 2003. Cloning of the full-length rhesus cytomegalovirus genome as an infectious and self-excisable bacterial artificial chromosome for analysis of viral pathogenesis. J. Virol. **77**:5073–5083.
6. **Chang WL, Kirchoff V, Pari GS, Barry PA.** 2002. Replication of rhesus cytomegalovirus in life-expanded rhesus fibroblasts expressing human telomerase. J. Virol. Methods **104**:135–146.
7. **Cohen JI, Moskal T, Shapiro M, Purcell RH.** 1996. Varicella in chimpanzees. J. Med. Virol. **50**:289–292.
8. **Ferenczi K, Burack L, Pope M, Krueger JG, Austin LM.** 2000. CD69, HLA-DR and the IL-2R identify persistently activated T cells in psoriasis vulgaris lesional skin: blood and skin comparisons by flow cytometry. J. Autoimmun. **14**:63–78.
9. **Gerdes J, et al.** 1984. Cell cycle analysis of a cell proliferation-associated human nuclear antigen defined by the monoclonal antibody Ki-67. J. Immunol. **133**:1710–1715.
10. **Gierasch WW, et al.** 2006. Construction and characterization of bacterial artificial chromosomes containing HSV-1 strains 17 and KOS. J. Virol. Methods **135**:197–206.
11. **Gomi Y, et al.** 2002. Comparison of the complete DNA sequences of the Oka varicella vaccine and its parental virus. J. Virol. **76**:11447–11459.
12. **Gray WL.** 2003. Pathogenesis of simian varicella virus. J. Med. Virol. **70**(Suppl 1):S4–S8.
13. **He J, et al.** 1997. CCR3 and CCR5 are co-receptors for HIV-1 infection of microglia. Nature **385**:645–649.
14. **Heininger U, Seward JF.** 2006. Varicella. Lancet **368**:1365–1376.
15. **International AIDS Vaccine Initiative.** 2012. Preventive AIDS vaccine candidates in human clinical trials. International AIDS Vaccine Initiative, New York, NY.
16. **Kader M, et al.** 2009. $\alpha4^+\beta7^{hi}CD4^+$ memory T cells harbor most Th-17 cells and are preferentially infected during acute SIV infection. Mucosal Immunol. **2**:439–449.
17. **Kirchoff V, Wong S, St JS, Pari GS.** 2002. Generation of a life-expanded rhesus monkey fibroblast cell line for the growth of rhesus rhadinovirus (RRV). Arch. Virol. **147**:321–333.
18. **Koropchak CM, et al.** 1991. Investigation of varicella-zoster virus infection by polymerase chain reaction in the immunocompetent host with acute varicella. J. Infect. Dis. **163**:1016–1022.
19. **Koropchak CM, Solem SM, Diaz PS, Arvin AM.** 1989. Investigation of varicella-zoster virus infection of lymphocytes by in situ hybridization. J. Virol. **63**:2392–2395.
20. **Krause PR, Klinman DM.** 2000. Varicella vaccination: evidence for frequent reactivation of the vaccine strain in healthy children. Nat. Med. **6**:451–454.
21. **Mainka C, Fuss B, Geiger H, Hofelmayr H, Wolff MH.** 1998. Characterization of viremia at different stages of varicella-zoster virus infection. J. Med. Virol. **56**:91–98.
22. **Martin KA, et al.** 1997. CD4-independent binding of SIV gp120 to rhesus CCR5. Science **278**:1470–1473.
23. **Messaoudi I, et al.** 2009. Simian varicella virus infection of rhesus macaques recapitulates essential features of varicella zoster virus infection in humans. PLoS Pathog. **5**:e1000657.
24. **Myers MG, Kramer LW, Stanberry LR.** 1987. Varicella in a gorilla. J. Med. Virol. **23**:317–322.
25. **Nagaike K, et al.** 2004. Cloning of the varicella-zoster virus genome as an infectious bacterial artificial chromosome in *Escherichia coli*. Vaccine **22**:4069–4074.
26. **Ohtaki S, Hondo R, Kodama H, Kurata T.** 1988. Experimental activation of latent cytomegalovirus infection of the captive bred (F1) cynomolgus monkeys by live or killed varicella-zoster virus inoculated under immunosuppression. Acta Pathol. Jpn. **38**:967–978.
27. **Ohtaki S, Kodama H, Hondo R, Kurata T.** 1986. Activation of cytomegalovirus infection in immunosuppressed cynomolgus monkeys inoculated with varicella-zoster virus. Acta Pathol. Jpn. **36**:1537–1552.
28. **Southwick CH, Siddiqi MF.** 1994. Population status of nonhuman primates in Asia, with emphasis on rhesus macaques in India. Am. J. Primatol. **34**:51–59.
29. **Staprans SI, et al.** 2004. Enhanced SIV replication and accelerated progression to AIDS in macaques primed to mount a CD4 T cell response to the SIV envelope protein. Proc. Natl. Acad. Sci. U. S. A. **101**:13026–13031.
30. **Takahashi M.** 1986. Clinical overview of varicella vaccine: development and early studies. Pediatrics **78**:736–741.
31. **Takahashi M.** 1984. Development and characterization of a live varicella vaccine (Oka strain). Biken J. **27**:31–36.
32. **Takahashi M.** 1996. The varicella vaccine. Vaccine development. Infect. Dis. Clin. North Am. **10**:469–488.
33. **Takahashi M, et al.** 2003. Enhancement of immunity against VZV by giving live varicella vaccine to the elderly assessed by VZV skin test and IAHA, gpELISA antibody assay. Vaccine **21**:3845–3853.
34. **Takahashi M, Otsuka T, Okuno Y, Asano Y, Yazaki T.** 1974. Live vaccine used to prevent the spread of varicella in children in hospital. Lancet **2**:1288–1290.
35. **ten Haaft P, et al.** 2001. Comparison of early plasma RNA loads in different macaque species and the impact of different routes of exposure on SIV/SHIV infection. J. Med. Primatol. **30**:207–214.
36. **Terada K, et al.** 2000. Low induction of varicella-zoster virus-specific secretory IgA antibody after vaccination. J. Med. Virol. **62**:46–51.
37. **Wang X, et al.** 2009. Monitoring $\alpha4\beta7$ integrin expression on circulating $CD4^+$ T cells as a surrogate marker for tracking intestinal $CD4^+$ T-cell loss in SIV infection. Mucosal Immunol. **2**:518–526.
38. **Willer DO, et al.** 2010. Multi-low-dose mucosal simian immunodeficiency virus SIVmac239 challenge of cynomolgus macaques immunized with "hyperattenuated" SIV constructs. J. Virol. **84**:2304–2317.